

Supporting information

Biodegradable prussian blue/manganese dioxide core-shell nanoparticles with open cages for imaging-guided chemo-photothermal combined therapy of cancer cells

Ying Gao^{a,1}, Jinbo Xue^{a,1}, Yuebo Yang^b, Dongxiao Bian^a, Luyao Liu^a, Ming Zhu^a, Tao Yang^{a,*}, Le Liu^{a,*}

¹Y.G. and J.X. contributed equally to this work.

^aDepartment of Stomatology, NO. 964 hospital of the chinese people's liberation army joint logistics support force, Jilin 130021, PR China, E-mail: 1595765865@qq.com, 1350288208@qq.com

^bNational University of Singapore, 21 Lower Kent Ridge Rd, 119077, Singapore

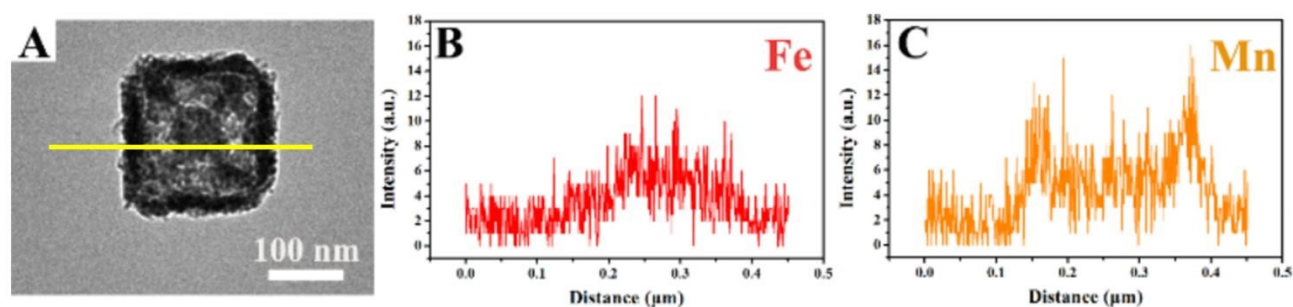


Fig S1. (A) TEM image of a single PBMn-5 NPs. (B-C) Elemental line scan analysis of PBMn-5 NPs.

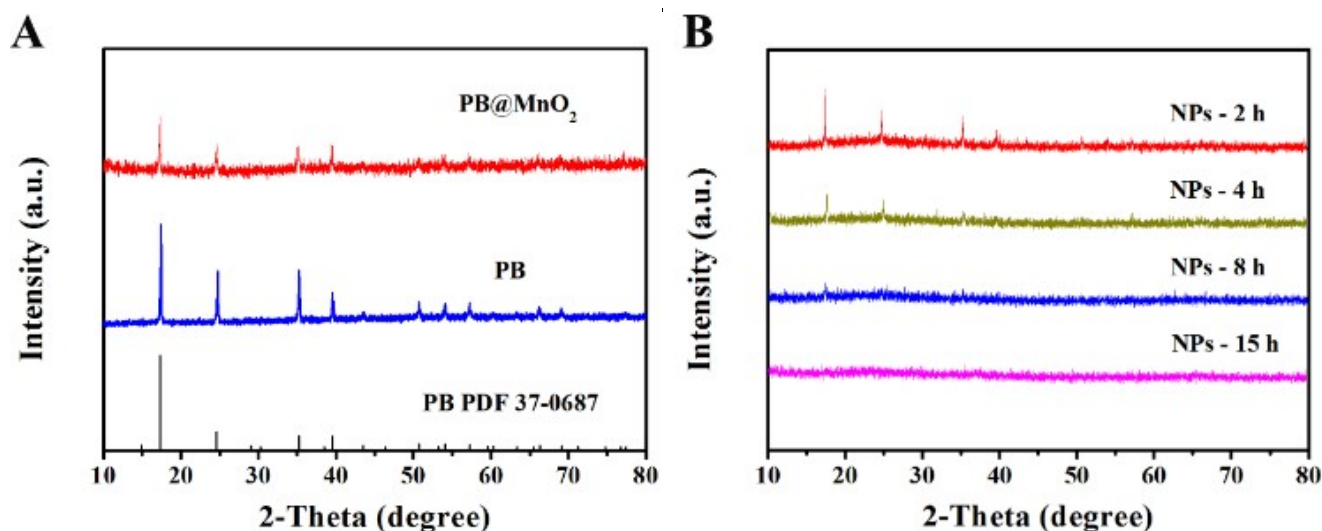


Fig S2. (A) XRD patterns of PB and PBMn-5 NPs. (B) XRD patterns of NPs with different reaction time (2, 4, 8, and 15 h).

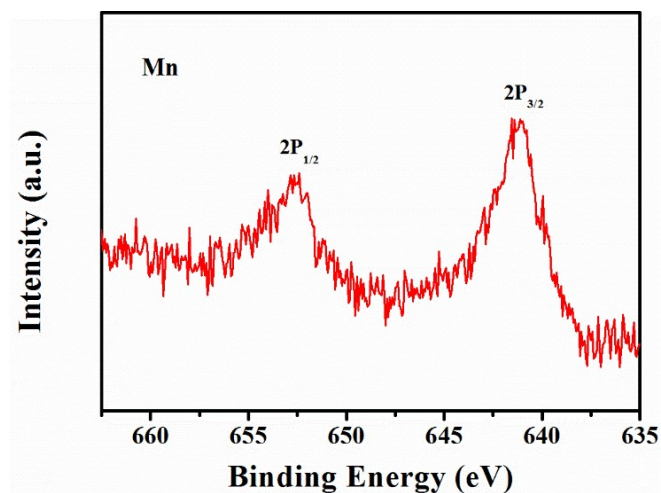


Fig S3. XPS spectrum of Mn elements in PBMn-5 NPs.

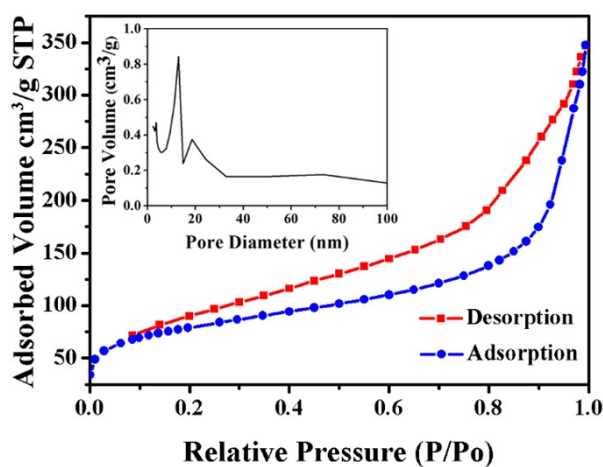


Fig S4. N₂ adsorption–desorption isotherms and pore-size distribution curve (inset) of the PBMn-5 NPs.

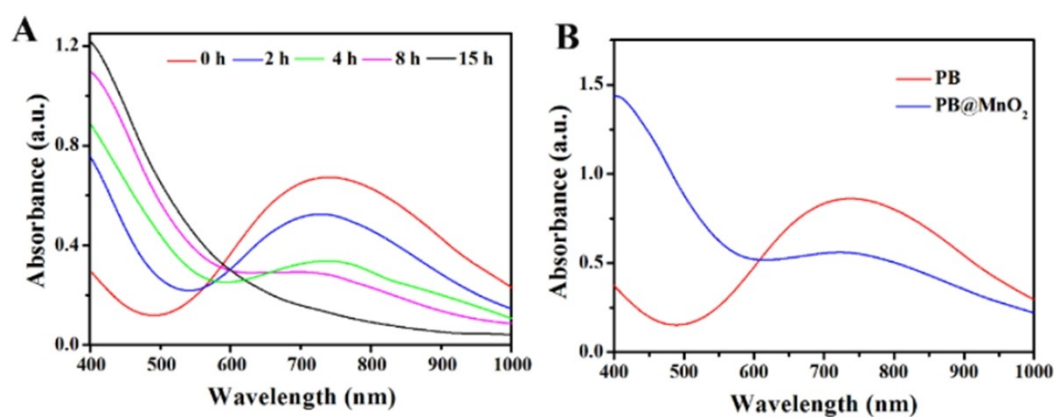


Fig S5. (A) UV-Vis absorption spectra of NPs with different reaction time (0, 2, 4, 8, and 15 h). (B) UV-Vis absorption spectra of PB NPs and PBMn-5 NPs.

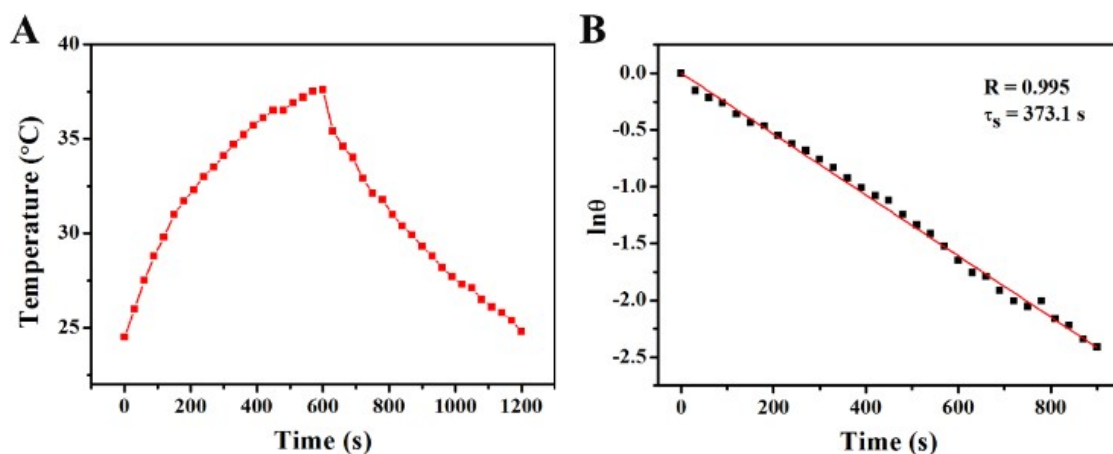


Fig S6. (A) Photothermal response of the aqueous dispersion of PBMn-5 NPs under NIR laser (808 nm, 1.0 W cm^{-2}) irradiation for 10 min. (B) Linear time date versus $-\ln\theta$ obtained from the cooling period.

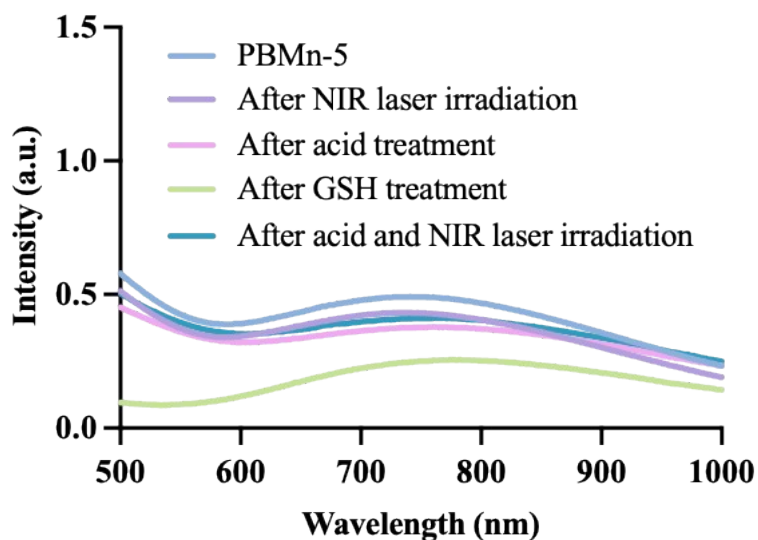


Fig S7. UV-Vis absorption spectra of PBMn-5 NPs after different treatment.

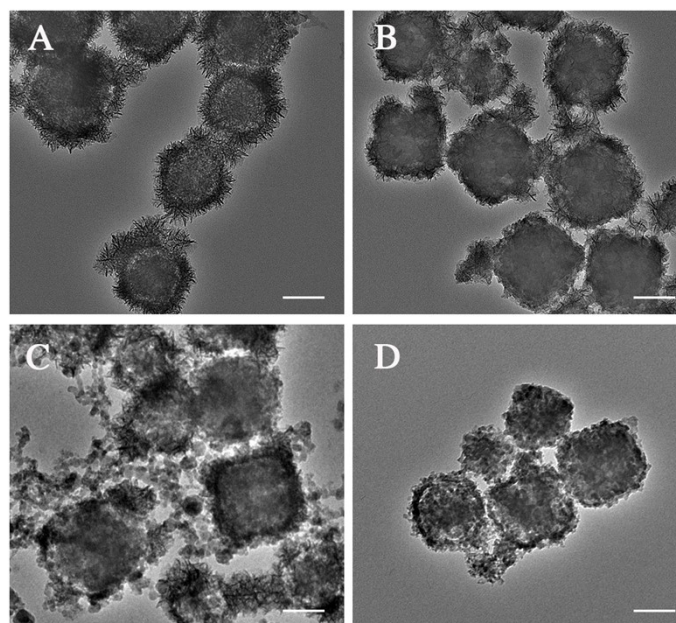


Fig S8. TEM images of PBMn-5 NPs (A) before and after treated with (B) NIR laser irradiation, (C) acidic PBS, and (D) GSH. The scale bar is 100 nm.

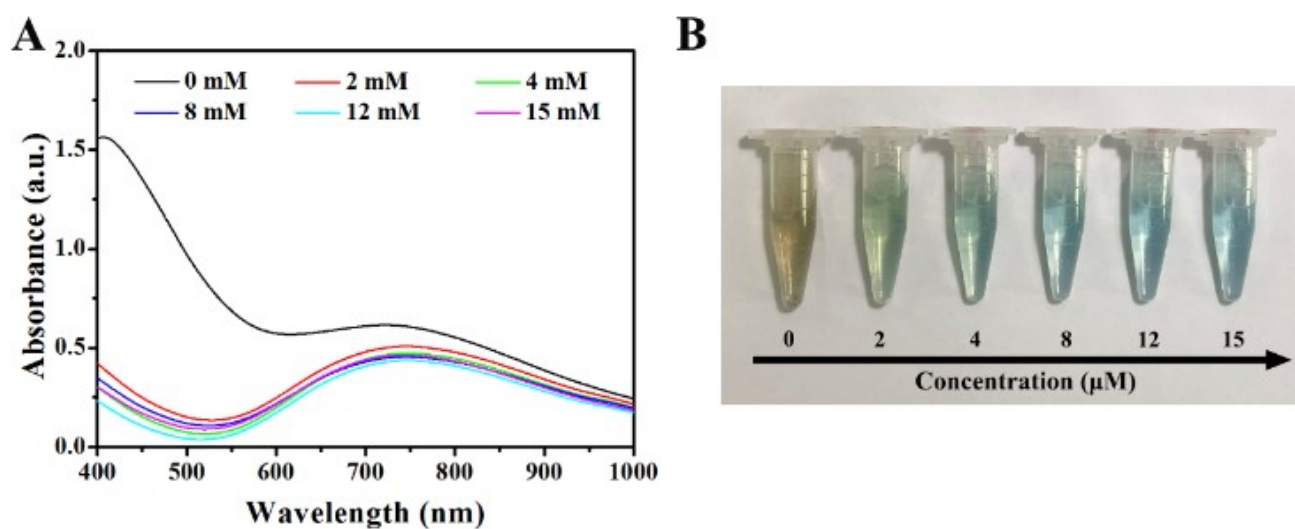


Fig S9. (A) UV-vis absorption spectra of PBMn-5 NPs after reaction with increased concentration of GSH. (B) Digital images of PBMn-5 NPs (0.1 mg mL^{-1}) after reaction with increased concentration of GSH.